ORIGINAL PAPER

Commissioning NIS 1 kN·m Primary Torque Standard Machine

K. M. Khaled* and G. A. Aggag

National Institute of Standards (NIS), Tersa Street, Haram, P.O. box 136, Giza 12211, Egypt

© The Author(s) 2022

Abstract: The presented work shows the design and evaluation of the NIS 1 kN·m primary torque standard machine. The machine covers the range up to 1000 N·m with a very wide range of torque steps thanking different 4 mass stacks. The machine has a double-side lever arm with half-moon ends to provide calibration in the clockwise and anticlockwise directions. An air bearing was used as a fulcrum to provide a low friction coefficient. FEA was used in the design and optimization process of the lever arm. The relative expanded uncertainty of the machine is 0.03% which is proved by recalibration of two reference torque transducers of 200 N·m and 1000 N·m capacity. All En values are less than unity, which reveals the competence of the developed machine.

Keywords: Torque; Calibration; Primary; Machine; Evaluation

1. Introduction

Years ago, the National Institute of Standards of Egypt (NIS) built a 3 kN·m secondary standard torque calibration machine [1, 2]. This machine was bilaterally compared with the KRISS machine, and the results were published [3]. Later on, NIS decided to build a 1 kN·m primary torque standard machine (1 kN·m-PTSM) with cooperation with PTB to provide torque traceability with lower uncertainty [4]. Many design approaches in many NMIs are reviewed to realize torque by primary meaning. PTB, the NMI of Germany, has primary machines with capacities from 1 to 20 kN·m, which uses a set of masses hanged by a double side lever arm floating over compressed air in an air bearing as a fulcrum [5–8]. The NMIJ, the NMI of Japan uses a similar technique to build its 1 kN·m machine while using two air bearings to suspend the lever arm of the 20 kN·m machine [9–11]. Sanponpute presents an idea to replace the aerostatic bearing with suspended-fulcrum from low capacity torque machines [12]. This paper presents the developed machine's design concept and evaluation process to reach an expected relative expanded uncertainty of 3×10^{-4}.
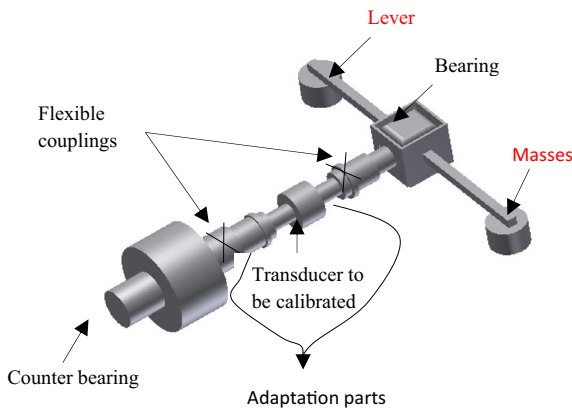
2. Design Concepts

Figure 1 shows the proposed main components of the machine. The machine has a double-side lever arm supported by an air bearing as a fulcrum. A set of masses are loaded onto one lever side to apply torque either in clockwise or anticlockwise directions. The calibrated torque transducer is assembled by hydraulic clamps and two flexible couplings to the machine shafts.

2.1. Lever Arm Design

The designed lever is a double-side lever arm with cylindrical coaxial ends which form a circle as shown in Fig. 2. The radius of curvature (r_c) of both ends is the lever arm length which is nominally equal to 1 m. A 130 μm thickness flexible metal belt is assembled to the upper part of the lever arm end (half-moon) and follow its profile to hang the loading frame. A set of dead weights are used to generate the applied forces. The contact point between the flexible metal belt and the half-moon is dependable on the horizontality of the lever arm to assure constant lever arm length even with lever arm inclination within the acceptable angles which is considered a privilege.
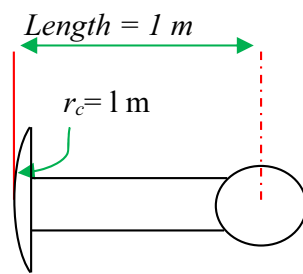
The designed lever is supposed to load up to 1 kN to achieve the machine target rated capacity of 1 kN·m. The datasheet of the selected air bearing state that the maximum capacity is 2.2 kN which includes the lever arm, cylindrical shaft, loading mechanism, weights, flexible

---

*Corresponding author, E-mail: khaled_fmmd_nis@yahoo.com

Fig. 1 Main parts of the 1 kN·m-PTSM

Table 1 Summary of the proposed 8 design models (codes from 3 to 10)

Model code	Weight (kg)	Approx. maximum stress (MPa)	End deflection (U1) (mm)
3	18.39	24.67	0.11
4	10.45	28.14	0.12
5	8.10	27.64	0.12
6	7.31	28.7	0.12
7	7.31	27.91	0.12
8	6.68	59.75	0.15
9	7.00	34.58	0.13
10	7.78	47.89	0.14

Fig. 2 Cylindrical coaxial lever arm

coupling, and hydraulic clamp. Different models of the lever arm are studied either rectangular cross section or I-beam cross section. Finite Element Analysis (FEA) software was used to test the proposed models. The stress and deformation of a simple AISI 304 I-beam cross-sectional cantilever model loaded by a 1 kN at the end were solved analytically and by the FEA software to get the best software settings. The initial element type was a 3-D Tet element deformable solid part. Different element sizes were used to check the dependency of the output stresses on the element size and found to exist. This test revolves that a Tet element of 35 mm size give relative errors of 0.1% and 2.5% for stress and deflection, respectively. The next step was to propose 8 different models to select the lowest deformation and the lightest weight among them. The first model is considered simple enough. Then, the FEA software was used to test to show the least stressed parts to use the optimization technique called Evolutionary Structural Optimization (ESO) to slowly remove the low-stress materials.

The elastic deformations and the corresponding stresses along with the lever arm are shown in Fig. 3. The elastic deformation is on the left y-axis opposite to the von misses stresses on the right y-axis while the distance from the centre of the air bearing towards the lever arm end is shown on the x-axis. Table 1 shows the maximum stresses, deformation, and corresponding weight. Figure 3 and

Fig. 3 FEA of the proposed 8 design models (codes from 3 to 10)
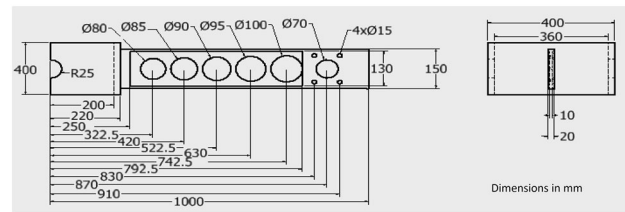
Fig. 4 Lever arm front and side views

Table 1 show that Model 7 gives less weight and the lowest stress among all models.

The detailed working drawings of the designed lever arm are shown in Fig. 4. Figure 5 shows that the von misses stress of the designed lever arm is 24.65 MPa (left) and the elastic deformation in the horizontal direction (U1) is 0.12 mm (right). Because this lever arm is symmetric about its neutral axis, under load the upper part is going to be lengthened by the same amount of lower part shortening. The value of the elastic deformation is considered important to be known because it means that the lever arm

Fig. 5 FEA of the lever arm, Von Misses stress on the (left) and the corresponding elastic deflection (U1) (right)
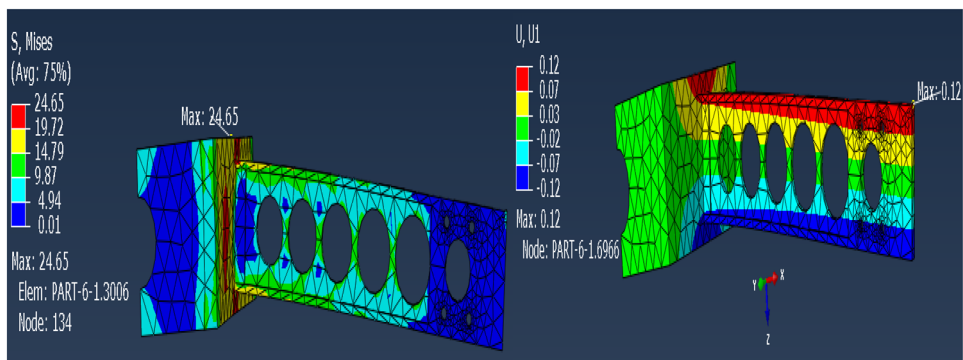

will be extended under load consequentially the applied torque.

To test the influence of the lever arm deflection on the machine accuracy, the FEA software was used to approximate the lever arm deflections in *x*-axis versus the applied forces from 25 N up to 1000 N. Figure 6 shows the applied force and the correspondence deflection and the machine error in N·m. This figure shows the predicted linear dependence between the applied force and the correspondence deflection. Furthermore, the values of the machine error started from − 0.000075 N·m at 25 N·m and move parabolic to reach − 0.12 N·m at 1000 N·m.

2.2. Lever Arm End Design and the Loading Frame

The lever arm length is the radius of curvature of the lever arm end (half-moon). The centre of this circle shape is the machine axis. The lever arm end is a hollow metal body with some weight reduction holes, and its outer surface forms a section of a circle. This end has to be slid over the
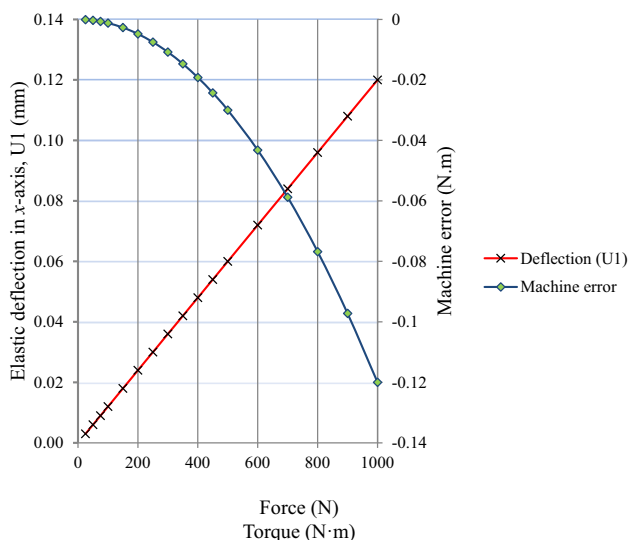
lever arm to reach the position to assemble the cover to the main lever arm end and the lever arm in between with 4 φ20 mm screws. Other 6 φ10 mm holes are used to assemble the cover to its main lever end as shown in Fig. 7. This design allows the machine lever arm length to be adjusted by 1 mm outward and inward.

A flexible metal belt is used that follows the shape of the circular surface section and is connected to the loading frame consisting of 2 columns and 2 upper and lower bridges to form this structure. The different weights can be loaded on the lower bridge as the lower bridge has a guide male cylinder. The design allows changing the contact area of the metal belt with the surface of the circular section, to maintain the length of the machine arm constant with the loading. Figure 8 shows the components and the assembly of the loading frame, while Fig. 9 shows the detailed design of the upper and lower symmetric bridges. This loading frame is symmetric about its vertical axis. This simple design offered easy loading and unloading of the weights.

Figure 10 shows the main parts of the designed lever arm and how weights will be loaded to the loading frame. This generated force will be transferred through the metal belt, lever arm end, the lever arm, rectangle box to the machine shaft and then finally to the torque transducer under calibration as a pure torque vector. Figure 11 shows a photograph of the NIS 1 kN·m primary torque standard machine.

3. Characteristics of the Developed Machine

This machine is designed to calibrate torque transducers with claimed relative expanded uncertainty of 3×10^{-4}. The uncertainty sources mainly come from force generation, length, and some other sources from the calibration conditions. A set of measurements were done to identify the uncertainty sources and their contribution. Finally, recalibration of 2 reference torque transducers was done to checkaine pformance with the claimed uncertainty. The
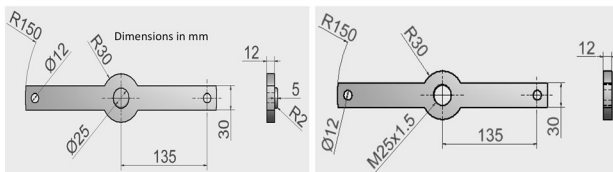

Fig. 6 FEA for the lever deflection and the corresponding machine error

Fig. 7 Detailed design of the lever arm end, main part (left) and the cover (right)
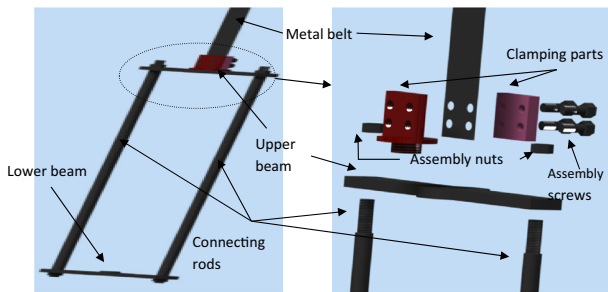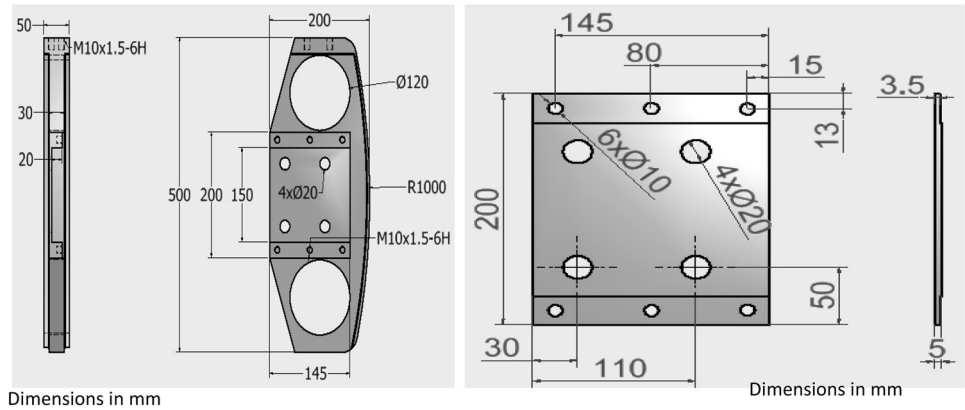
Fig. 8 Components of the loading frame

Fig. 9 Schematic of the lower beam (left) and the upper beam (right), of the loading frame
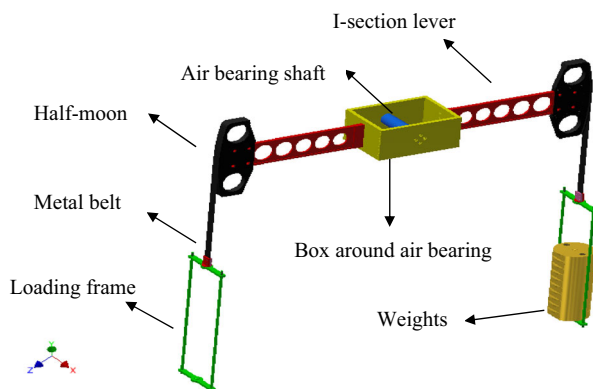
Fig. 10 Schematic of the developed lever-mass system

following equation is the model equation to realize torque by the primary method:

Fig. 11 NIS 1 kN·m primary torque standard machine

$$T = mgl\left(1 - \frac{\rho_{air}}{\rho_{mass}}\right) \qquad (1)$$

where T is the torque (N·m), m is the mass of the hanged weights (kg), g is the local gravitational acceleration (m/s^2), l is the perpendicular lever arm length (m), ρ_{air} is air density (kg/m^3), and ρ_{mass} is the mass material density (kg/m^3).

3.1. Uncertainty Source to Force (w_{force})

The realization of force values generated by weights is related to the local gravity value and its correction due to air buoyancy. The local gravity (g_{local}) is 9.7929917 m/s^2 with relative standard uncertainty (w_{grav}) less than 2×10^{-7} including the influence of tide and gravity gradient. The air buoyancy gives a relative standard uncertainty (w_{buoy}) of less than 2×10^{-6} at ambient conditions (21.6 °C $\pm$ 0.5 K, (43 $\pm$ 5) % and (988.3 $\pm$ 0.25) mbar). The measured local gravity value is used to control the weights within the machine uncertainty limits.

The austenitic stainless steel AISI 304 is used to build all weights. To cover a wide range of torque steps, 4 weight stacks each of 10 identical weights were manufactured. The

first weight stack is 50 N·m capacity with 5 N·m/weight. The second mass stack is 200 N·m capacity with 20 N·m/weight. The third weight stack is 500 N·m with 50 N·m/weight. The fourth mass stack is 1000 N·m capacity with 100 N·m/weight.

To adjust the weights, 2 threaded holes suitable in dimension for each stack were made on the top of each weight to control the weight during calibration. Thin solid threaded covers are used to cover these holes. The relative deviations are calculated for each weight and taken into consideration as a source of uncertainty as tabulated in Table 2.

3.2. Uncertainty Due to Arm Length (w_{length})

The lever arm length of each side is considered the distance between the centre of the machine axis and the middle of each flexible metal belt. As a fact, the lever arm length will be changed with loading weights. Moreover, the imperfection of the curvature of the lever arm ends will affect the lever arm length if the lever arm is inclined. The uncertainty contribution of a nominal thermal expansion coefficient of 1.6×10^{-5}/K and the lever arm inclination up to 10 degrees are tabulated in Table 2. One of the expected influencing parameters is the lever arm thermal expansion which should be taken into consideration. The whole lever arm parts were installed in their position onto the machine and then the length measurements were carried out using a laser tracker device.

3.3. Other Sources of Uncertainty (Sensitivity)

The developed machine uses an air bearing to support the lever arm and work as a fulcrum. The dependency of the machine's actual torque values and the effect of changing the air pressure on the bearing friction coefficient was studied using different capacity torque transducers and found to be very small compared to the machine's claimed uncertainty. The air bearing working pressure is 6 bar, which enables the air bearing used to withstand 2.5 kN as a

Table 2 Uncertainty budget of the developed machine

Error parameter (x_i)	Estimated value	Unit	Distribution	Sensitivity coefficient	Relative standard estimated uncertainty ($w(x_i)$)
Gravity acceleration	0.00002	%	Normal	1	0.00002
Air buoyancy force	0.00020	%	Normal	1	0.00020
Mass[1] (1000 N·m mass stack)	0.00040	%	Normal	1	0.00040
Mass[2] (500 N·m mass stack)	0.00302	%	Normal	1	0.00302
Mass[3] (200 N·m mass stack)	0.00115	%	Normal	1	0.00115
Mass[4] (50 N·m mass stack)	0.00338	%	Normal	1	0.00338
Friction coefficient	0.0002	%	Rectangular	1	0.0001
Change of the lever arm length due to inclination angle up to $\pm 10°$	0.002	%	Rectangular	1	0.0014
Change of the lever arm length due to half-moon perpendicularity	0.003	%	Rectangular	1	0.0019
Change of the lever arm length under load	0.025	%	Rectangular	1	0.0144
Change of the lever arm length due to thermal expansion up to ± 1 °C	0.0016	%	Rectangular	1	0.0009
Effect of air bearing pressure stability	0.001	%	Rectangular	1	0.0006
Relative standard estimated uncertainty[1] w (1000 N·m)		%			0.015
Relative standard estimated uncertainty[2] w (500 N·m)		%			0.015
Relative standard estimated uncertainty[3] w (200 N·m)		%			0.015
Relative standard estimated uncertainty[4] w (50 N·m)		%			0.015
Relative expanded measurement uncertaity[1] W (1000 N·m)		%			0.03
Relative expanded measurement uncertaity[2] W (500 N·m)		%			0.03
Relative expanded measurement uncertaity[3] W (200 N·m)		%			0.03
Relative expanded measurement uncertaity[4] W (50 N·m)		%			0.03

Table 3 Recalibration results of the 1000 N·m torque transducer

	Applied torque	Average TORQUE	Relative repeatability	Relative reproducibility	Relative expanded uncertainty	Class
	N·m	mV/V	(%)	(%)	(%)	
Measurements of the clockwise direction	0	–	–	–	–	–
	100	0.161920	0.002	0.004	0.03	0.2
	200	0.323858	0.002	0.004	0.03	0.2
	300	0.485778	0.002	0.014	0.03	0.2
	400	0.647721	0.003	0.011	0.03	0.2
	500	0.809672	0.002	0.007	0.03	0.2
	600	0.971611	0.005	0.008	0.03	0.2
	700	1.133561	0.004	0.006	0.03	0.2
	800	1.295522	0.004	0.006	0.03	0.2
	900	1.457474	0.002	0.003	0.03	0.2
	1000	1.619422	0.002	0.004	0.03	0.2
Measurements of anticlockwise direction	0	–	–	–	–	–
	100	− 0.161922	0.004	0.004	0.04	0.2
	200	− 0.323872	0.002	0.009	0.04	0.2
	300	− 0.485804	0.005	0.012	0.04	0.2
	400	− 0.647766	0.002	0.014	0.03	0.2
	500	− 0.809727	0.001	0.012	0.03	0.2
	600	− 0.971682	0.001	0.009	0.03	0.2
	700	− 1.133633	0.000	0.007	0.03	0.2
	800	− 1.295589	0.001	0.006	0.03	0.2
	900	− 1.457533	0.000	0.004	0.03	0.2
	1000	− 1.619490	0.001	0.003	0.03	0.2

radial force. The use of a dryer to remove water from the pressurized air has instant pressure drop up to 0.5 bar for about 5 s and recover again which causes instability of signal up to 25 nV/V for those 5 s.

To investigate the air bearing friction, a 50 N·m reference torque transducer connected to DMP 40 measuring amplifier, is assembled to the machine shafts and then a set of very small masses are added to the mass stack to change the readings by 0.00001 N·m at 0 N·m, 5 N·m, and 50 N·m. This test was repeated by a 1000 N·m reference torque transducer at (0, 50, 100, 200, 300, 400, 500, 600, 700, 800, 1000) N·m to make a 0.00005 N·m signal change. This investigation revealed that 10 mg mass can change the readings of the 50 N·m torque transducer by 0.00001 N·m, and a 50 mg mass can change the readings of the 1000 N·m torque transducer by 0.00001 N·m.

Table 2 shows the uncertainty budget of the developed machine for the 4 mass stacks used. The results revealed that the 3×10^{-4} relative expanded uncertainty could be achieved for all mass stacks.

4. Comparison of the machine

A set of recalibrations of 2 reference torque transducers, these torque transducers have a capacity of 1000 N·m and 200 N·m. The selected reference torque transducers have a continuous 5 repetitive calibrations at PTB with less than 0.002% relative drift error, which is decisive to ensure stability. The selected reference torque transducers are classified as 0.05 as per DIN 51,309 form 10% of the rated capacity. The recalibrations were carried out at (10%, 20%, 30%, 40%, 50%, 60%, 80%, and 100%) of the full scale in both clockwise and anticlockwise directions according to DIN 51,309 and the relative repeatability, reproducibility, and zero-point deviations are mainly the uncertainty sources. The loading time needed for the PTB machine to move from one step to the next one is strictly followed. Furthermore, the temperature and humidity corrections due to the environmental conditions' differences between the two labs and their influences on the transducer are taken into consideration. Tables 3 and 4 show the recalibration results of the 1000 N·m and the 200 N·m torque transducers, respectively. Table 3 shows that maximum relative expanded uncertainty in clockwise and anticlockwise

**Table 4** Recalibration results of the 200 N·m torque transducer

	Applied −torque N·m	Average torque mV/V	Relative repeatability (%)	Relative reproducibility (%)	Relative Expanded Uncertainty (%)	Class
Measurements of the clockwise direction	0	–	–	–	–	–
	20	0.158716	0.003	0.003	0.09	0.2
	40	0.317542	0.000	0.001	0.06	0.2
	60	0.476394	0.013	0.001	0.04	0.2
	80	0.635218	0.009	0.002	0.03	0.2
	100	0.794103	0.005	0.008	0.03	0.2
	120	0.952987	0.013	0.002	0.03	0.2
	140	1.111816	0.010	0.001	0.03	0.2
	160	1.270630	0.014	0.005	0.03	0.2
	180	1.429447	0.013	0.006	0.03	0.2
	200	1.588212	0.009	0.000	0.03	0.2
Measurements of anticlockwise direction	0	–	–	–	–	–
	20	− 0.158687	0.009	0.057	0.08	0.2
	40	− 0.317536	0.002	0.029	0.04	0.2
	60	− 0.476331	0.037	0.031	0.04	0.2
	80	− 0.635167	0.028	0.024	0.04	0.2
	100	− 0.793945	0.025	0.034	0.04	0.2
	120	− 0.952680	0.011	0.005	0.03	0.2
	140	− 1.111494	0.012	0.010	0.03	0.2
	160	− 1.270303	0.005	0.006	0.03	0.2
	180	− 1.429073	0.011	0.003	0.03	0.2
	200	− 1.587758	0.010	0.010	0.03	0.2

Table 5 Comparison results of the 1000 N·m torque transducer

Calibration step N·m	NIS values		PTB values		$|En\text{-value}|$	Status
	Mean value (x_1) mV/V	Expanded uncertainty ($W(x_1)$) mV/V	Assigned value (x_{pt}) mV/V	Expanded uncertainty of the assigned value ($W(x_{pt})$) mV/V		
100	0.161920	0.000049	0.161915	0.000011	0.1	Satisfactory
200	0.323858	0.000099	0.323851	0.000016	0.1	Satisfactory
300	0.485778	0.000164	0.485783	0.000034	0.0	Satisfactory
400	0.647721	0.000208	0.647724	0.000026	0.0	Satisfactory
500	0.809672	0.000253	0.809668	0.000032	0.0	Satisfactory
600	0.971611	0.000303	0.971642	0.000058	0.1	Satisfactory
800	1.295522	0.000395	1.295525	0.000052	0.0	Satisfactory
1000	1.619422	0.000489	1.619443	0.000049	0.0	Satisfactory
− 100	− 0.161922	0.000070	− 0.161921	− 0.000005	0.0	Satisfactory
− 200	− 0.323872	0.000114	− 0.323851	− 0.000010	0.2	Satisfactory
− 300	− 0.485804	0.000173	− 0.485797	− 0.000015	0.0	Satisfactory
− 400	− 0.647766	0.000218	− 0.647755	− 0.000026	0.0	Satisfactory
− 500	− 0.809727	0.000262	− 0.809709	− 0.000024	0.1	Satisfactory
− 600	− 0.971682	0.000305	− 0.971674	− 0.000029	0.0	Satisfactory
− 800	− 1.295589	0.000395	− 1.295596	− 0.000039	0.0	Satisfactory
− 1000	− 1.619490	0.000488	− 1.619549	− 0.000065	0.1	Satisfactory

Table 6 Comparison results of the 200 N·m torque transducer

Calibration step N·m	NIS values		PTB values		|En-value|	Status
	Mean value (x_1) mV/V	Expanded uncertainty $(W(x_1))$ mV/V	Assigned value (x_{pt}) mV/V	Expanded uncertainty of the assigned value $(W(x_{pt}))$ mV/V		
20	0.158716	0.000139	0.158770	0.000010	0.4	Satisfactory
40	0.317542	0.000178	0.317551	0.000010	0.0	Satisfactory
60	0.476394	0.000172	0.476336	0.000019	0.3	Satisfactory
80	0.635218	0.000213	0.635115	0.000019	0.5	Satisfactory
100	0.794103	0.000251	0.793911	0.000024	0.8	Satisfactory
120	0.952987	0.000299	0.952695	0.000029	1.0	Satisfactory
160	1.270630	0.000404	1.270253	0.000038	0.9	Satisfactory
200	1.588212	0.000492	1.587818	0.000064	0.8	Satisfactory
− 20	− 0.158687	0.000120	− 0.15877	− 0.000011	0.7	Satisfactory
− 40	− 0.317536	0.000121	− 0.317553	− 0.000019	0.1	Satisfactory
− 60	− 0.476331	0.000213	− 0.476318	− 0.000014	0.1	Satisfactory
− 80	− 0.635167	0.000254	− 0.635115	− 0.000025	0.2	Satisfactory
− 100	− 0.793945	0.000334	− 0.793897	− 0.000032	0.1	Satisfactory
− 120	− 0.952680	0.000311	− 0.952698	− 0.000038	0.1	Satisfactory
− 160	− 1.270303	0.000407	− 1.270256	− 0.000038	0.1	Satisfactory
− 200	− 1.587758	0.000516	− 1.587831	− 0.000048	0.1	Satisfactory

(100-1000) N·m calibration steps in Clockwise direction
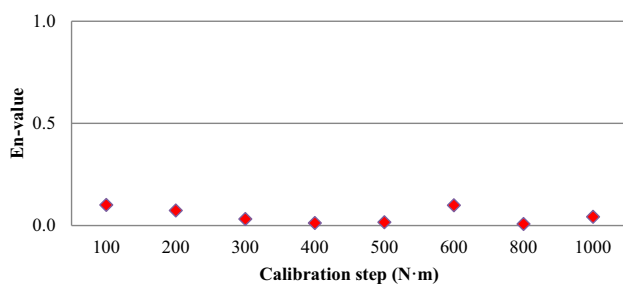
Fig. 12 *En*-values for the 1000 N·m transducer in a clockwise direction

(100-1000) N·m calibration steps in Anticlockwise direction
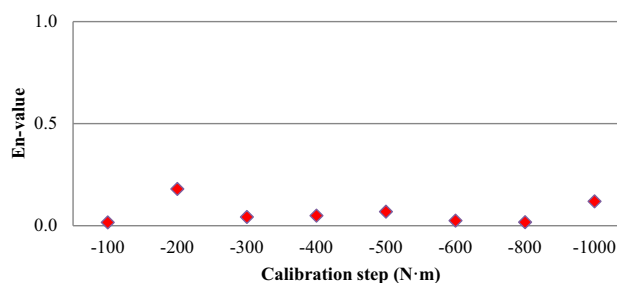
Fig. 13 *En*-values for the 1000 N·m transducer in the anticlockwise direction

directions are 0.03% and 0.04%, respectively, and the 0.2 class is achievable from 100 N·m. While Table 4 shows that the maximum relative expanded uncertainty in clockwise and anticlockwise directions are 0.09% and 0.08%, respectively, and the 0.2 class is also achievable from 20 N·m.

Tables 5 and 6 show the comparison results of the 1000 N·m and the 200 N·m torque transducers, respectively in clockwise and anticlockwise directions.

The Normalized error technique (En) is used to evaluate the competency of the machine as it is one of the trusted evaluation techniques in calibration laboratories. The assigned value in each torque measurement point is the average value presented in the last calibration certificate issued by PTB. Figures 12, 13, 14 and 15 show a graphical representation of the En values for both torque transducers from 20 N·m up to 1000 N·m in both directions. All En values from 20 N·m up to 1000 N·m in clockwise and anticlockwise directions are below unity, which reveals that all NIS measurements are consistent within their uncertainties.

(20-200) N·m calibration steps in Clockwise direction
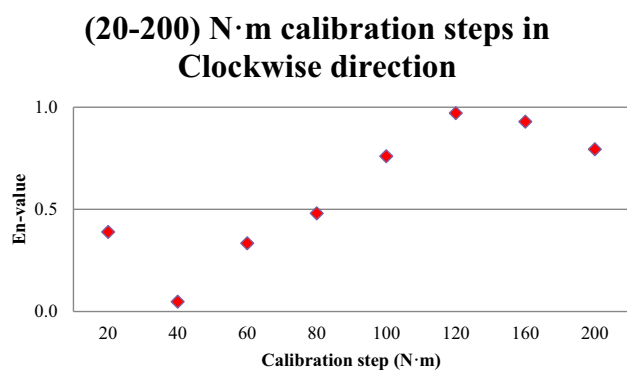
Fig. 14 *En*-values for the 200 N·m transducer in the clockwise direction

(20-200) N·m calibration steps in Anticlockwise direction
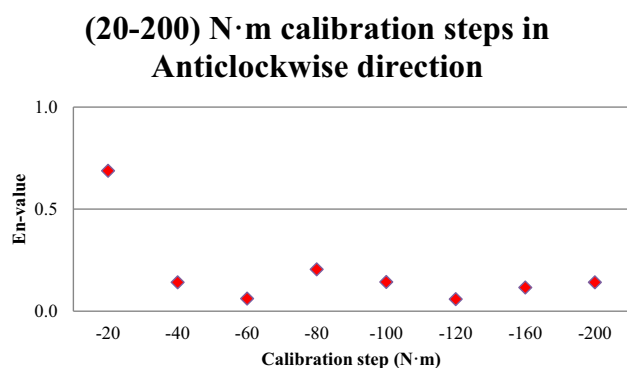
Fig. 15 *En*-values for the 200 N·m transducer in the anticlockwise direction

5. Conclusion

NIS 1 kN·m primary torque standard machine was built at NIS with 4 mass stacks to cover the torque range from 5 N·m up to 1000 N·m. The machine has a double-side lever arm to provide calibration in clockwise and anti-clockwise directions. An air bearing was used as a fulcrum to provide a low friction coefficient. FEA was used in the design and optimization process of the lever arm. Different uncertainty sources were studied, and the 0.03% machine relative expanded uncertainty was proved via a recalibration of two very stable reference torque transducers to cover the range from 20 N·m up to 1000 N·m as the En values are less than unity. An international comparison is planned for the next year.

References

[1] K.M. Khaled, G.A. Aggag, A.E. Abuelezz and M.G. Elsherbiny, Mechanical design of NIS new reference torque standard machine, IMEKO 2010 TC3, TC5 and TC22 conferences metrology in modern context, Pattaya, (2009) pp. 109–114.

[2] K.M. Khaled, G.A. Aggag, A.E. Abuelezz and M.G. Elsherbiny, Performance evaluation of NIS new reference torque standard machine, IMEKO 2010 TC3, TC5 and TC22 conferences metrology in modern context, Pattaya, (2009) pp. 269–272.

[3] M.-S. Kim and K.M. Khaled, Torque key comparison CCM.T-K1.3. measurand torque: 0 N m, 500 N m, 1000 N m, Metrologia, **52** (2015) 07007.

[4] K.M. Khaled, Design, development and calibration of torque standard machine, PhD Thesis. Faculty of Engineering, Cairo University, (2016).

[5] C. Schlegel, D. Röske, D. Mauersberger and P. Hohmann, Metrological characterization of a 20 N·m torque calibration standard machine at PTB, Germany. J. Phys. Conf. Ser., **1065** (2018) 042026. https://doi.org/10.1088/1742-6596/1065/4/042026.

[6] D. Röske, Metrological characterization of a 1 N m torque standard machine at PTB, Germany, Metrologia, **51** (2014) 87–96. http://iopscience.iop.org/0026-1394/51/1/87/

[7] D. Peschel, Proposal for the design of torque calibration machines using the principle of a component system, proceedings of the 15th IMEKO TC3 conference, Madrid, (1996) pp. 251–254.

[8] K. Adolf, D. Mauersberger and D. Peschel, Specifications and uncertainty of measurement of the PTB's 1 kNm torque standard machine, proceedings of the 14th IMEKO TC3 conference, Warsaw, (1995) pp. 174–176.

[9] K. Ohgushi, T. Tojo and A. Furuta, Development of the 1 kN m torque standard machine, proceedings of the XVI IMEKO world congress, vol. 3, Vienna, (2000) pp. 217–223.

[10] K. Ohgushi, T. Ota, K. Ueda and E. Furuta, Design and development of the 20 kN·m deadweight torque standard machine, proceedings of the 18th IMEKO TC3 conference, Celle, (2002) pp. 52–57, Code 108601. https://www.imeko.org/publications/tc3-2002/IMEKO-TC3-2002-009.pdf

[11] K. Ohgushi, T. Ota and K. Ueda, Uncertainty evaluation of the 20 kN m deadweight torque standard machine, proceedings of the 19th international conference IMEKO TC-3, Cairo, (2005) CD-ROM.

[12] T. Sanponpute, P. Chantaraksa, N. Saenkhum and N. Arksonnarong, Suspended-fulcrum torque standard machine, XIX IMEKO world congress, Lisbon, (2009) pp. 343–346.